

# Investigations of structure and transport in lithium and silver borophosphate glasses

Sundeeep Kumar,<sup>a</sup> Philippe Vinatier,<sup>b</sup> Alain Levasseur,<sup>b</sup> and K.J. Rao<sup>a,\*</sup>

<sup>a</sup>Solid State and Structural Chemistry Unit, Material Research Center, Indian Institute of Science, Bangalore 560012, India

<sup>b</sup>Groupe Ionique du Solide, ENSCPB, University of Bordeaux I, Avenue Pey Berland, BP 108 33402 Talence Cedex, France

Received 12 October 2003; received in revised form 10 December 2003; accepted 30 December 2003

## Abstract

Glasses in the system  $x\text{Li}_2\text{O} \cdot (1-x)[0.5\text{B}_2\text{O}_3 \cdot 0.5\text{P}_2\text{O}_5]$  and  $x\text{Ag}_2\text{O} \cdot (1-x)[0.5\text{B}_2\text{O}_3 \cdot 0.5\text{P}_2\text{O}_5]$  have been prepared from melt quenching method. Glasses have been characterized for their densities, molar volumes, glass transition temperatures and heat capacities. Structural studies have been done using infrared and high resolution magic angle spinning nuclear magnetic resonance (HR MAS NMR) of  $^{31}\text{P}$ ,  $^{11}\text{B}$  and  $^7\text{Li}$  nuclei. Boron is present only in tetrahedral coordination except in  $\text{Li}_2\text{O}$ -rich glasses. Transport properties have been investigated over a wide range of frequency and temperature. Silver containing glasses are found to possess higher conductivities and lower barriers than lithium containing glasses. A structural model has been proposed in which pure  $\text{B}_2\text{O}_3$ – $\text{P}_2\text{O}_5$  compositions are assumed to be constituted of  $\text{BPO}_4$  units and modification occurs selectively on the phosphate moiety. Tetrahedral boron units are thus expected to be retained in the glass structure.

© 2004 Elsevier Inc. All rights reserved.

**Keywords:** Borophosphate glasses;  $\text{BPO}_4$  glass; NBO–BO switching and tetrahedral boron

## 1. Introduction

The most common glasses generally consist of more than one glass former (typically  $\text{SiO}_2$ ,  $\text{B}_2\text{O}_3$ ,  $\text{P}_2\text{O}_5$ ) with modifier metal oxides. The oxygen from the metal oxide becomes part of the covalent glass network creating new structural units. In the process the polymeric structure is partially broken down and this depolymerization or modification of the glass network increases the range of compositions, which can be studied in glassy state. The cations of the modifier oxide are generally present in the neighborhood of the nonbridging oxygens (NBO) in the glass structure. The extent of network modification obviously depends upon the concentration of modifier oxide present in the glass. The depolymerization of glass network affects various physical properties such as density, molar volume,  $T_g$ , heat capacity etc. The ‘fragilities’ of the melts from which the glass is prepared also increases upon modification because the network dimensionality decreases [1]. Since  $F_{1/2}$  fragilities are determined by measured thermodynamic quantities,  $F_{1/2}$

in turn can be related to the concentration of modifier oxide and during the process of conduction they diffuse through the modified glass network [1]. Since both the magnitude of conduction and fragility depend upon the extent of modification,  $F_{1/2}$  and conductivity are also expected to be interrelated.

Borophosphate glasses possess a variety of useful properties. Alkali and silver borophosphate glasses are fast ion conductors [2,3]. Several borophosphates exhibit high chemical durability. Borophosphate glass structure has very interesting features.  $^{11}\text{B}$  NMR spectroscopic investigations by Yun and Bray [4] have revealed that borophosphate glasses contain both  $\text{BO}_3$  and  $\text{BO}_4$  structural units. Yun and Bray [4] also concluded that the glass structure contain  $\text{BPO}_4$  units.  $\text{BPO}_4$  units have unique structure in which  $[\text{BO}_{4/2}]^-$  tetrahedral units are structurally coupled to  $[\text{PO}_{4/2}]^+$  tetrahedral units. The negative charge on  $[\text{BO}_4]^-$  is compensated by the positive charge on  $[\text{PO}_4]^+$  so that the twinned unit of  $\text{BPO}_4$  as a whole is neutral. Crystalline boron phosphate is constituted of  $\text{BPO}_4$  units. The presence of only  $\text{BPO}_4$  units in borophosphate glasses has been further supported by studies of chemical durability and variations of  $T_g$  in

\*Corresponding author. Fax: +90-80-3601310.

E-mail address: [kjr Rao@sscu.iisc.ernet.in](mailto:kjr Rao@sscu.iisc.ernet.in) (K.J. Rao).

borophosphate glasses by Kreidl and Weil [5] and by Takahashi [6]. The formation of  $\text{BPO}_4$  has also been indicated in the ESR studies [7] of cesium borophosphate glasses and infrared studies [8] of potassium borophosphate glasses. Koudelka and Mosner [9,10] have studied zinc borophosphate and zinc-lead borophosphate glasses and found that addition of  $\text{B}_2\text{O}_3$  increases  $T_g$  and attributed it to increased crosslinking and hence the dimensionality of the network. In Raman spectra there was conspicuous absence of the  $808\text{ cm}^{-1}$  band suggesting the absence of boroxol rings. IR spectra revealed the presence of P–O–B linkages.

Nevertheless the presence of  $\text{BPO}_4$  units in borophosphate glasses has not been universally supported. Ducl et al. [11,12] have investigated  $\text{NaPO}_3\text{--Na}_2\text{B}_4\text{O}_7$  glasses over a wide range of compositions using infrared, Raman,  $^{31}\text{P}$  and  $^{11}\text{B}$  MAS NMR. In their  $^{31}\text{P}$  MAS and  $^{11}\text{B}$  NMR spectra, there was no clear evidence of the presence of  $\text{BPO}_4$  units. Lithium and silver borophosphate glasses have been thoroughly investigated by Chiodelli and coworkers [2,3,13,14] using wide range of techniques. While their Raman spectra indicate the presence of  $\text{BPO}_4$ , no definitive evidence was found in  $^{31}\text{P}$  MAS NMR. These authors concluded that borophosphate glasses may consist of P–O–B linkages, but not the  $\text{BPO}_4$  units. It has also been observed that ionic conductivities in borophosphate glasses are higher than that in corresponding binary borate and phosphate glasses.

Therefore, structures of borophosphate glasses require to be further investigated. A hypothetical glass of equimolar  $\text{B}_2\text{O}_3$  and  $\text{P}_2\text{O}_5$  with the formula  $\text{BPO}_4$  can be assumed to be structurally analogous to  $\text{SiO}_2$  glass in which half each of the silicon atoms in  $\text{SiO}_2$  in the network are alternately replaced by B and P atoms.  $\text{BPO}_4$  structure therefore consists of twinned  $[\text{PO}_{4/2}]^+$  and  $[\text{BO}_{4/2}]^-$  tetrahedral units in the structure. Unlike in ultraphosphate glasses,  $[\text{POO}_{3/2}]^0$  groups have become  $\text{PO}_{4/2}^+$  groups so that effectively there are only two oxygen atoms associated with each phosphorus atom. Structurally the situation is as if the double bond in  $[\text{POO}_{3/2}]^0$  has opened up enabling phosphorus to be associated with four bridging oxygens (BO).  $[\text{BO}_{4/2}]^-$  is widely known to occur in all alkali modified borate glasses, but in  $\text{BPO}_4$  and several crystalline borates, boron is present in  $[\text{BO}_{4/2}]^-$  groups. In the hypothetical  $\text{BPO}_4$  glass, therefore, one would expect the presence of a chemically ordered structure, in so that  $\text{B}_4^-$  ( $\equiv\text{BO}_{4/2}$ ) and  $\text{P}_4^+$  ( $\equiv\text{PO}_{4/2}$ ) are present in exclusive connectivity to each other;  $\text{B}_4^-$  connected only to  $\text{P}_4^+$  and vice versa. Therefore, there can be only B–O–P bonds in such a glass. B–O–B or P–O–P bonds are expected to be present only in  $\text{B}_2\text{O}_3$  or  $\text{P}_2\text{O}_5$  rich compositions respectively. Indeed Bray and coworkers [4] have provided the spectroscopic evidence for such chemical ordering.

The process of modification implies making available additional  $\text{O}^{2-}$  for degradation (depolymerization) of the network. It is interesting to ask how does the modification affect the  $\text{BPO}_4$  structure, which consists of only B–O–P bonds because we would normally expect both B–O $^-$  and P–O $^-$  types of NBO to result from modification. B–O $^-$  cannot form in a  $[\text{BO}_{4/2}]^-$  as it is well-known that NBO's are never present in a tetrahedral boron in glasses. Therefore, it appears as if both NBO's may eventually form as P–O $^-$ . Further, when  $[\text{PO}_{4/2}]^+$  groups take up additional  $\frac{1}{2}$  ( $\text{O}^{2-}$ ) during modification they are expected to return to the ultraphosphate structure  $[\text{POO}_{3/2}]^0$ . It would therefore appear that the modifier has not affected the less acidic borate groups in the network and has modified only the more acidic phosphate part of the network. There are also other structural implications, when one considers bond (BO) auditing after modification. The resulting structure can be expected to influence ion transport in the glasses in a major way. Therefore, we consider the investigation of borophosphate glasses containing equimolar  $\text{B}_2\text{O}_3$  and  $\text{P}_2\text{O}_5$  as extremely interesting.

In this article, we report wide range of structural investigations and transport studies on lithium and silver borophosphate glasses. Two glass series, namely  $\text{Li}_2\text{O--B}_2\text{O}_3\text{--P}_2\text{O}_5$  (LBP series) and  $\text{Ag}_2\text{O--B}_2\text{O}_3\text{--P}_2\text{O}_5$  (ABP series) have been prepared with equal quantities of  $\text{B}_2\text{O}_3$  and  $\text{P}_2\text{O}_5$  (ratio of unity) in the glass composition. Their physical properties such as densities and molar volumes, thermal properties like heat capacity and glass transition temperatures have been analyzed. Infrared and magic angle spinning nuclear magnetic resonance (MAS NMR) (of  $^{31}\text{P}$ ,  $^{11}\text{B}$  and  $^7\text{Li}$  nuclei) spectroscopies have been used to analyze the structure and suggest a viable structural model. Transport properties have been investigated over wide ranges of temperatures and frequencies and discussed in the context of the suggested structural model.

## 2. Experimental

Glasses were prepared by the conventional melt quenching method. The starting materials,  $\text{Li}_2\text{CO}_3$  (Qualigens) ( $\text{Ag}_2\text{O}$  (Qualigens)),  $(\text{NH}_4)_2\text{HPO}_4$  (Aldrich) and  $\text{H}_3\text{BO}_3$  (Qualigens) (all of Analar grade) were mixed thoroughly by grinding in appropriate quantities so as to constitute a 10 g batch. The ground mixtures were heated in platinum crucibles at 673 K for about 5 h in a muffle furnace in order to decompose  $\text{Li}_2\text{CO}_3$  and  $(\text{NH}_4)_2\text{HPO}_4$ . The batches were then melted at 1573 K for about 10 min, stirred to ensure homogeneity and quenched between stainless steel plates kept at room temperature.

The amorphous nature of the glass samples was confirmed using X-ray diffraction ( $\text{CuK}\alpha$  Siemens

D-5005, Germany). Using Differential Scanning Calorimetry (DSC) (Perkin-Elmer DSC-2), glass transition temperature,  $T_g$  and heat capacity,  $C_p$  of the samples were determined. Dry nitrogen was used as purge gas during DSC experiments. The  $C_p$  of the glasses was determined from room temperature up to temperatures well above  $T_g$  (till crystallization temperature) using corresponding DSC data on single crystal sapphire ( $\text{Al}_2\text{O}_3$ ) (standard). The densities were determined using glass bits free of air bubbles and cracks (in  $10\times$  magnification) using apparent weight loss method with xylene as the immersion fluid. Measured densities of well-annealed glasses were found to be accurate and reproducible to  $\pm 0.001\text{ g/cm}^3$ . The molar volumes,  $V_m = (W_m/\text{density})$ , were calculated from density data,  $W_m$  being the corresponding formula weights.

The Fourier transform infrared (FTIR) spectra of the glasses were recorded between  $4000\text{ cm}^{-1}$  and  $400\text{ cm}^{-1}$  on a Nicolet 740 FTIR spectrometer. KBr pellets containing the samples were used for the purpose.  $^{31}\text{P}$ ,  $^{11}\text{B}$  and  $^7\text{Li}$  (116.590 MHz) spectra were recorded on a Bruker MSL-300 solid-state high-resolution spectrometer operating magnetic field 7.05 T.  $90^\circ$  pulses of  $5\mu\text{s}$  were employed with a delay time of 10 s between pulses in all the experiments. A spinning speed of 7–10 kHz was employed. All the spectra were recorded at room temperature using freshly powdered samples. Trimethyl boron was used as a standard for recording  $^{11}\text{B}$  NMR.

Electrical conductivity measurements were carried out on a Hewlett-Packard HP 4192A LF impedance-gain phase analyzer (Hewlett-Packard, USA) from 10 Hz to 13 MHz in the temperature range of 298–600 K. A home built cell assembly (having a 2-terminal capacitor configuration and silver electrodes) was used for the measurements. The sample temperature was measured using a Pt–Rh thermocouple positioned very close to the sample. The temperature was controlled using a Heatcon (Bangalore, India) temperature controller and the temperature constancy of  $\pm 1\text{ K}$  was achieved in the entire range of measurements. Annealed circular glass bits, coated with silver paint on both sides having thickness of about 0.1 cm and 1 cm diameter were used for measurements. The real ( $Z'$ ) and imaginary ( $Z''$ ) parts of the complex impedance ( $Z^*$ ) were obtained from the measured conductance and capacitance using the standard relations between  $Z'$  and  $Z''$  with  $G$  and  $C$  ( $G$  is the conductance,  $C$  is parallel capacitance respectively) at various frequencies ( $\omega$ ). The real ( $\epsilon'$ ) and imaginary ( $\epsilon''$ ) parts of the complex dielectric constant were calculated from the relations  $\epsilon' = Cd/\epsilon_0 A$  and  $\epsilon'' = \sigma/\omega\epsilon_0$ , where  $d$  is the sample thickness,  $A$  is the cross-sectional area,  $\sigma$  is the conductivity, and  $\epsilon_0$  is the permittivity of free space.

The data were also analyzed using the electrical modulus formalism. The real ( $M'$ ) and imaginary ( $M''$ )

parts of the complex electrical modulus ( $M^* = 1/\epsilon^*$ ) were obtained from  $\epsilon'$  and  $\epsilon''$  values using the relation,

$$M' = \frac{\epsilon'}{(\epsilon')^2 + (\epsilon'')^2}$$

and

$$M'' = \frac{\epsilon''}{(\epsilon')^2 + (\epsilon'')^2}.$$

### 3. Results and discussion

The glasses have been made with constant  $\text{B}_2\text{O}_3$  to  $\text{P}_2\text{O}_5$  ratio of unity. Two series of glasses have been made: first,  $x\text{Li}_2\text{O} \cdot (1-x)[0.5\text{B}_2\text{O}_3 \cdot 0.5\text{P}_2\text{O}_5]$  (LBP series) and the second,  $x\text{Ag}_2\text{O} \cdot (1-x)[0.5\text{B}_2\text{O}_3 \cdot 0.5\text{P}_2\text{O}_5]$  (ABP series). The compositions of the glasses along with their codes are shown in Table 1.

#### 3.1. Densities and molar volumes

The densities and molar volumes of all the glasses are listed in Table 2. The variation of densities of both the series are shown in Fig. 1(a) as a function of  $\text{Li}_2\text{O}$  and  $\text{Ag}_2\text{O}$  concentrations. Densities in LBP series show a slightly monotonically decreasing trend as a function of  $\text{Li}_2\text{O}$  mole fraction, whereas in ABP series densities increase as  $\text{Ag}_2\text{O}$  mole fraction increases. The decrease in the density in LBP series is from 2.465 to 2.419  $\text{g/cm}^3$  and the density increase in ABP series from 3.70 to 5.0  $\text{g/cm}^3$  in the composition regime studied here. The effect of addition  $\text{Li}_2\text{O}$  and  $\text{Ag}_2\text{O}$  on the variation of molar volumes of the glasses is shown in Fig. 1(b) for both the series. The molar volumes in both the series decrease as the modifier ( $\text{Li}_2\text{O}$  or  $\text{Ag}_2\text{O}$ ) concentration increases. The magnitudes of decrease in molar volumes in the range of (30–50) mol% addition are 5.64 and 4.69  $\text{cm}^3$  for LBP and ABP series respectively. The slight difference between volume changes between LBP and ABP series of glasses reflects the influence of the smaller

Table 1  
The compositions of glasses along with their codes

Codes	$\text{Li}_2\text{O}$	$\text{B}_2\text{O}_3$	$\text{P}_2\text{O}_5$
LBP1	30	35	35
LBP2	35	32.5	32.5
LBP3	40	30	30
LBP4	45	27.5	27.5
LBP5	50	25	25
	$\text{Ag}_2\text{O}$	$\text{B}_2\text{O}_3$	$\text{P}_2\text{O}_5$
ABP1	30	35	35
ABP2	35	32.5	32.5
ABP3	40	30	30
ABP4	45	27.5	27.5
ABP5	50	25	25

Table 2  
Densities, molar volumes,  $T_g$ ,  $C_P$  ( $T_g - 20$ )K,  $\Delta C_P$  and  $F_{1/2}$  values

Glass	Density (g/cm <sup>3</sup> )	Molar volume (cm <sup>3</sup> )	$T_g$ (K)	$C_P$ at ( $T_g - 20$ )K	$\Delta C_P$	$F_{1/2}$
LBP1	2.465	33.68	730	112.6	73.5	0.52
LBP2	2.457	32.24	717	111.3	60.3	0.65
LBP3	2.449	30.80	702	107.4	61.3	0.47
LBP4	2.432	29.45	692	105.3	52.3	0.47
LBP5	2.419	28.04	695	98.5	56.6	0.5
ABP1	3.710	38.70	727	107.5	86.6	0.44
ABP2	3.845	38.98	697	103.5	76.9	0.33
ABP3	4.166	37.49	668	99.1	80.3	0.32
ABP4	4.681	34.71	620	83.8	47.1	0.41
ABP5	4.962	34.01	590	83.4	51.3	0.38

size  $\text{Li}^+$  ion compared to that of the  $\text{Ag}^+$  ion on the resulting molar volumes.

### 3.2. Thermal studies

The glass transition temperatures ( $T_g$ ), heat capacity,  $C_P$  at ( $T_g - 20$ )K,  $\Delta C_P$  and thermodynamic fragility values are listed in Table 2. The variation of  $T_g$  as a function of modifier content is shown in Fig. 2 for both the series.  $T_g$  decreases as the extent of modification increases in both the cases. The decrease in  $T_g$  is rather dramatic in the case of ABP series where  $T_g$  decreases roughly 130 K as  $\text{Ag}_2\text{O}$  content is increased from 30 to 50 mol%. The decrease in  $T_g$  in LBP series is somewhat moderate and the magnitude of decrease is roughly 40 K over the same 20 mol%  $\text{Li}_2\text{O}$ . But it is somewhat surprising that glasses with 30 mol%  $\text{Li}_2\text{O}$  or  $\text{Ag}_2\text{O}$ , both have similar values of  $T_g$ . Since  $T_g$  dependence on composition is quite complex, extrapolation of the  $T_g$  towards pure  $\text{BPO}_4$  glass would not be meaningful. However, the large drop in  $T_g$  is indicative of a pronounced softening of the glass framework in the ABP glasses.

Thermodynamic fragilities,  $F_{1/2}$  were evaluated [15] using the expression  $F_{1/2} = (0.151 - x)/(0.151 + x)$ , where  $x = \Delta T_g/T_g$ ;  $\Delta T_g$  being the width of the glass transition. These fragilities are listed in Table 2. The observed differences in the magnitudes of  $F_{1/2}$  in LBP and ABP glasses imply that the structures of the corresponding melts are indeed affected by the cations ( $\text{Li}^+$  and  $\text{Ag}^+$ ) also. The observation that ABP glasses are more fragile than LBP glasses although  $\Delta C_P$  in  $\text{Li}_2\text{O}$  modified glasses is higher, is nevertheless unusual, because higher  $\Delta C_P$  implies higher degree of ionicity and generally such glasses are also associated with higher values of  $F_{1/2}$ . The origin of this behavior is unclear to us.

### 3.3. Spectroscopic studies: infrared

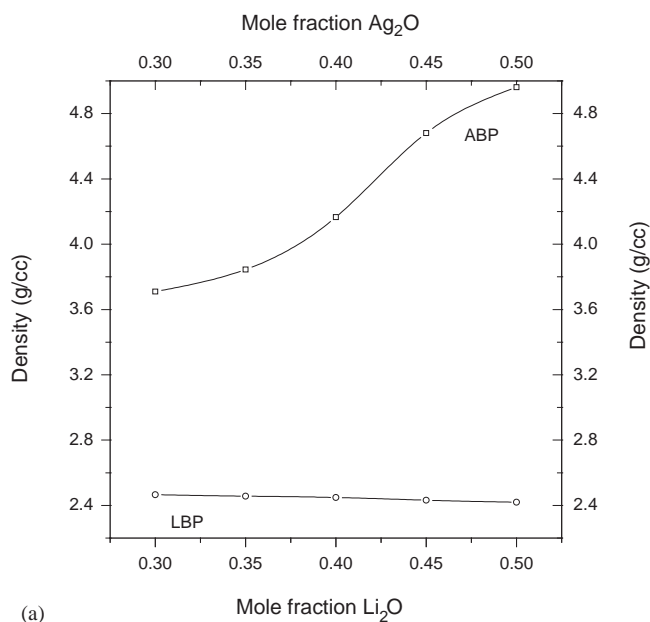
Spectra of both series of glasses are shown in Fig. 3. In the region of  $1400\text{ cm}^{-1}$  where trigonal boron

vibrations are expected, there is a gradual build up of intensity as we go from LBP1 to LBP5. The build up is clearly evident in the ABP5 spectrum. The absorption band near  $1200\text{ cm}^{-1}$  can be ascribed [16–18] to  $\text{P}=\text{O}$  vibrations and its relative intensity (compare with  $\sim 1000\text{ cm}^{-1}$  peak) increases. It also broadens and red shifts towards the highly modified LBP 5 composition. Absorption band around  $1045\text{ cm}^{-1}$  may be attributed to symmetrical stretching in both  $\text{PO}_4$  and  $\text{BO}_4$  groups. The relatively weaker absorption band at  $840\text{ cm}^{-1}$  can be assigned to the symmetric stretching vibrations ( $\text{P}-\text{O}-\text{B}$ ) linkages. This absorption gradually loses intensity towards LBP5 and ABP5 compositions. Simultaneously there is the increase of intensity of the  $950\text{ cm}^{-1}$  band, which can be ascribed to  $\text{B}-\text{O}-\text{B}$  stretching modes. The bending modes of  $\text{PO}_4$  and  $\text{P}-\text{O}-\text{B}$  contribute together to the bands in the range of  $450\text{--}600\text{ cm}^{-1}$ .

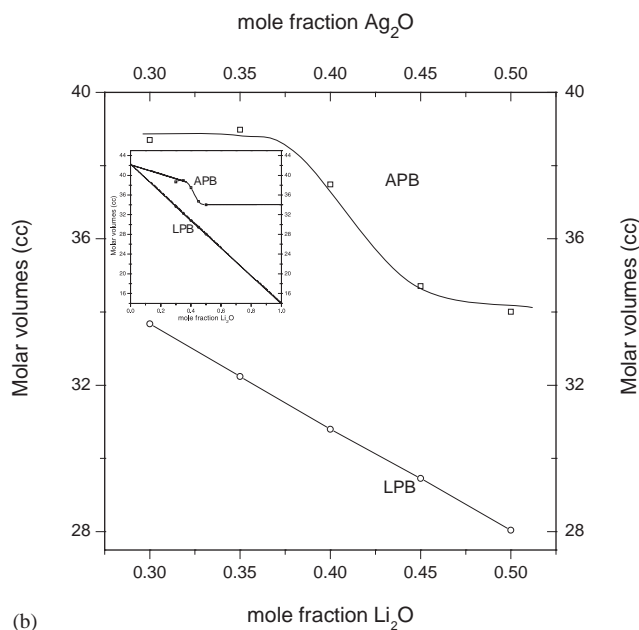
### 3.4. HR MAS NMR

Spectra of  $^{31}\text{P}$ ,  $^{11}\text{B}$  and  $^7\text{Li}$  have been analyzed and the chemical shifts are listed in Table 3.  $^{31}\text{P}$  MAS NMR spectra are shown in Fig. 4 for both the series of glasses. In LBP glasses,  $^{31}\text{P}$  chemical shift values lie in the range of  $-1$  to  $-20$  ppm. Although the range of chemical shifts observed here correspond to the known range of chemical shifts of meta and pyrophosphates, it is difficult to assign them precisely as the peaks in the spectra are undifferentiated in LBP glasses. However, the spectra of ABP glasses (ABP3, ABP4 and ABP5) indicate the presence of two peaks and hence two species. Thus in LBP glasses, the NMR peaks are broader and undifferentiated where as they are differentiated in high  $\text{Ag}_2\text{O}$ —ABP glasses.  $^{11}\text{B}$  MAS NMR for both the series are shown in Fig. 5. The  $^{11}\text{B}$  NMR has been used to calculate the fraction of tetrahedral boron and the calculated [1]  $N_4$  values ( $N_4 = B_4/(B_3 + B_4)$ ), (where  $B_3$  is itself the number of  $[\text{BO}_{3/2}]^0$ ,  $[\text{BO}_{2/2}\text{O}]^-$  and  $[\text{BO}_{1/2}\text{O}_2]^{2-}$  and  $B_4$  is  $B_4^-$  or  $[\text{BO}_{4/2}]^-$ ) are listed in Table 3 for all the 10 glasses. It is found that  $N_4$  is very high (nearly unity) for LBP1, LBP2, ABP1 and ABP2 glasses. Presence of significant





(a)



(b)

Fig. 1. (a) Variation of density in LBP and ABP series of glasses as a function of mole fraction of modifier oxide and (b) variation of molar volume of LBP and ABP series of glasses as a function of mole fraction of modifier oxide. The inset to Fig. 1(b) shows the extrapolation towards hypothetical  $\text{BPO}_4$  glass (left side) and pure  $\text{Li}_2\text{O}$  and pure  $\text{Ag}_2\text{O}$  (right side).

fraction of trigonal borons is evidenced only when  $\text{Li}_2\text{O}$  or  $\text{Ag}_2\text{O}$  concentration is high (nearly 50 mol%).  $^7\text{Li}$  MAS NMR is also shown in Fig. 6 for LBP series. The chemical shift values are listed in Table 3 along with  $^{31}\text{P}$  chemical shifts.  $^7\text{Li}$  chemical shifts are calculated using  $\text{LiCl}$  (aq. sol) as standard.  $\text{Li}^+$  ions appear to be slightly more deshielded in glasses compared to  $\text{Li}^+$  ions in the standard  $\text{LiCl}$  solution.

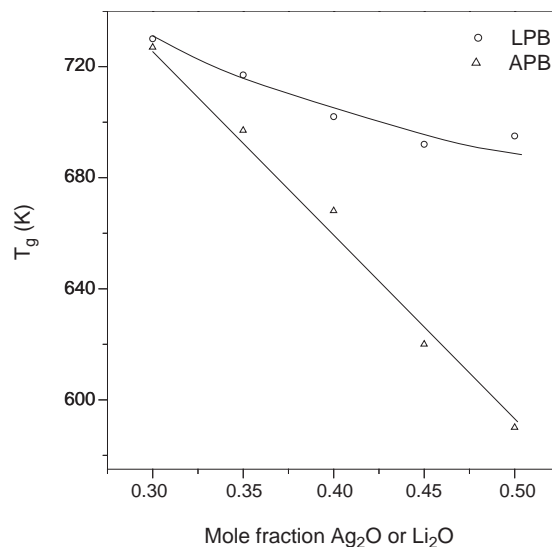


Fig. 2. Variation of glass transition temperatures of LBP and ABP series of glasses as a function of modifier oxide concentration.

### 3.5. Conductivity and relaxation studies

AC conductivity measurements have been performed on the samples over wide ranges of frequencies and temperatures. Inset to Fig. 7 is a Nyquist plot for the case of ABP5 glass at 263 K. DC conductivity has been calculated using the low frequency intercept on the X-axis. Fig. 7 illustrates the Arrhenius behavior of DC conductivities for a representative case of LBP3 glass. Fig. 7 reveals that the Arrhenius plot of the DC conductivity is quite linear. The solid line in the figure shows a typical Arrhenius fit to the data from which the activation energy is calculated. The DC conductivities at 363 K and the activation barriers ( $E_{\text{dc}}$ ) are listed in Table 4 for all the 10 glasses. Conductivities of ABP glasses are higher in magnitude than those of corresponding in LBP glasses. The activation barriers are plotted in Fig. 8 as a function of modifier concentration. Activation barriers decrease in both series of glasses as modifier concentration is increased although the decrease in LBP glasses is far less steep than in ABP glasses.

AC conductivity has been analyzed using Almond-West [19–21] single exponent power law,  $\sigma(\omega) = \sigma(0) + A\omega^s$ , where  $\sigma(0)$  is zero frequency conductivity,  $A$  is a constant,  $s$  is power law exponent and  $\omega$  the angular frequency. Log–log plot of  $\sigma$  vs  $\omega$  is shown for the case of LBP2 glass in Fig. 9 at various temperatures (Fig. 9(a)). The solid line in Fig. 9(a) is the fit to Almond-West power law for the data at 313 K. The fitting parameters are given in Table 5 for LBP2 glass at various temperatures. The power law fit is found to be remarkably good.  $s$  values obtained from fitting have been plotted in Fig. 9(b) for all the glasses as a function

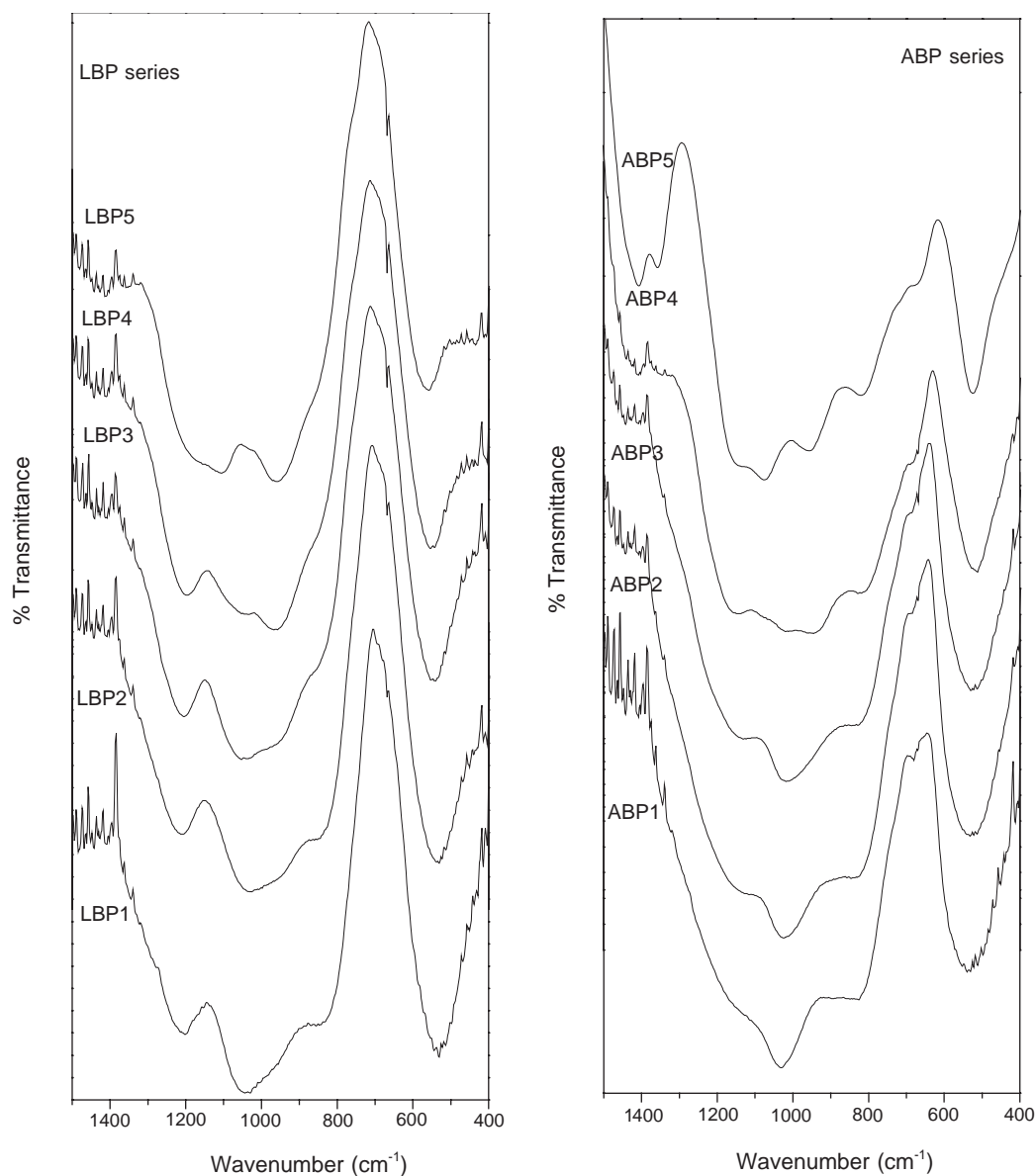


Fig. 3. The infrared spectra of LBP (left) and ABP (right) series of glasses.

Table 3  
Chemical shift values for  $^{31}\text{P}$  and  $^7\text{Li}$  MAS NMR along with calculated  $N_4$  values

Glass	$^{31}\text{P}$	$^7\text{Li}$	$N_4$	$P_4^+$	$P_2^-$
LBP1	-19.9	-1.1	1.0	40	30
LBP2	-16.0	-1.0	0.81	30	35
LBP3	-11.9	-0.9	0.72	20	40
LBP4	-8.9	-0.8	0.75	10	45
LBP5	-1.9	-0.7	0.73	0	50
ABP1	-18.9		1.0	40	30
ABP2	-19.1		1.0	30	35
ABP3	-16.0		1.0	20	40
	-5.3				
ABP4	-2.3		1.0	10	45
	12.3				
	-16.3				
ABP5	-1.2		0.83	0	50
	12.8				

of temperature. The  $s$  values essentially lie in the range of 0.60–0.65, which is typical of conductors in Jonscher regime [22]. There is no evidence of any minima or maxima in the behavior of  $s$ .

Conductivity data have also been analyzed using dielectric modulus formalism. The imaginary part ( $M''$ ) of complex moduli is shown in Fig. 10(a) as a function of frequency,  $f$  ( $\equiv \omega/2\pi$ ; as is generally done) on a semi-logarithmic plot at various temperatures.  $M''$  values exhibit peaks in the frequency domain. The  $M''$  peaks are asymmetric and broad which is characteristic of glasses. Assuming that  $M''$  peaks can be fitted to the conventional Kohlrausch-Williams-Watts (KWW) function [23–25] (the stretched exponential function), the full-width-at-half-maximum (FWHM) of the  $M''$  peaks have been used to calculate [26–27]  $\beta$  values. The

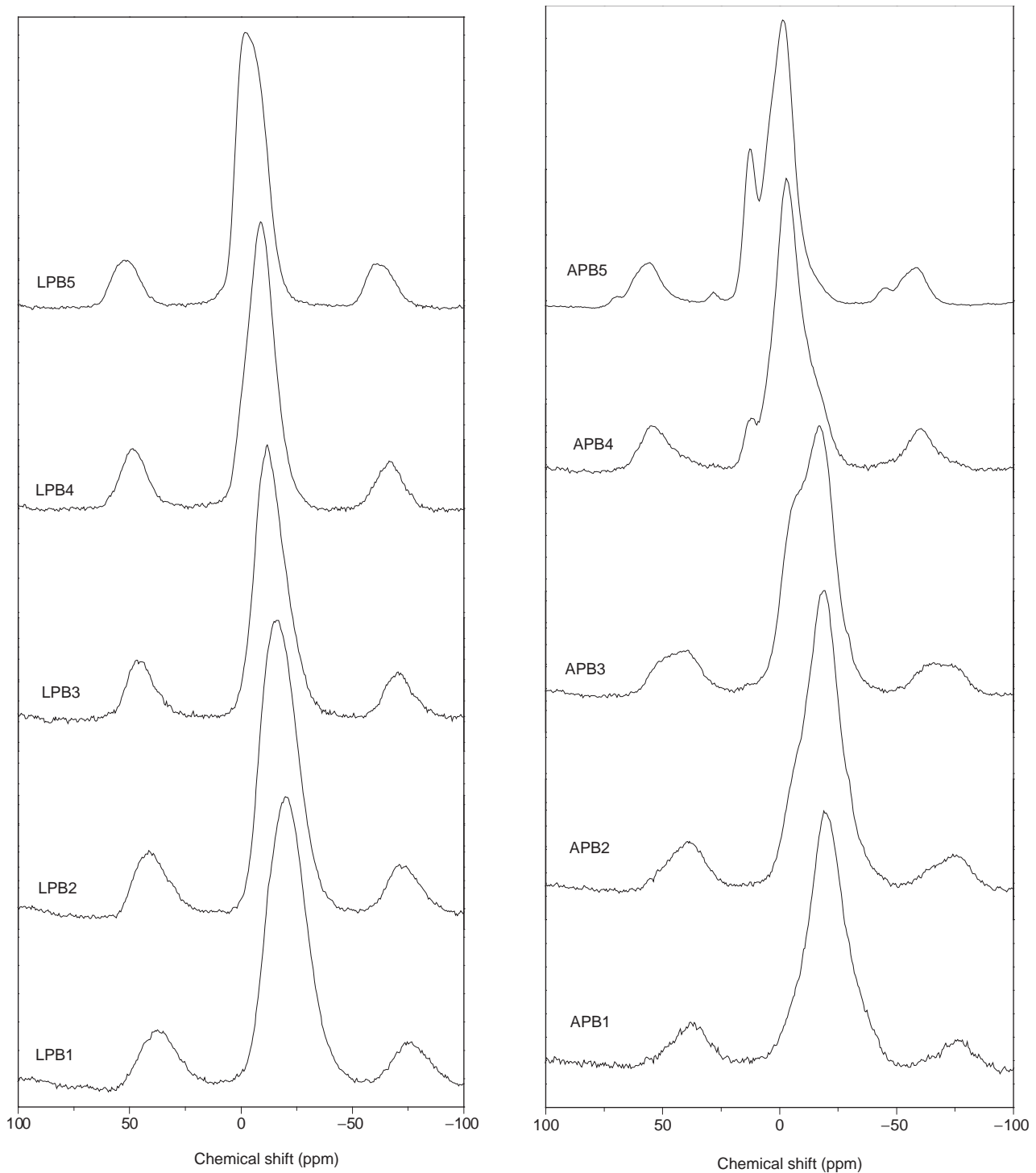


Fig. 4.  $^{31}\text{P}$  MAS NMR spectra of LBP and ABP glasses.

variation of  $\beta$  as a function of temperature is shown in Fig. 10 (b) for all the glasses.  $\beta$  values are around 0.52 and have been found to be independent of temperature.

The conductivity and modulus data have been found to satisfy time–temperature superposition. Fig. 11 (a) shows a plot of  $\log \sigma(\omega)/\sigma_{\text{dc}}$  vs  $\log (\omega/\omega_0)$  for the case of LBP2 glass and Fig. 11(b) shows a plot of

$M''/M''_{\text{max}}$  vs  $\log (f/f_0)$  for the same glass. The collapse of data in both the plots is very good, implying a common transport mechanism, which operates in the entire temperature range in all compositions. The carrier concentrations are rather high and do not permit examining conductivity scaling [28–30] in greater detail.

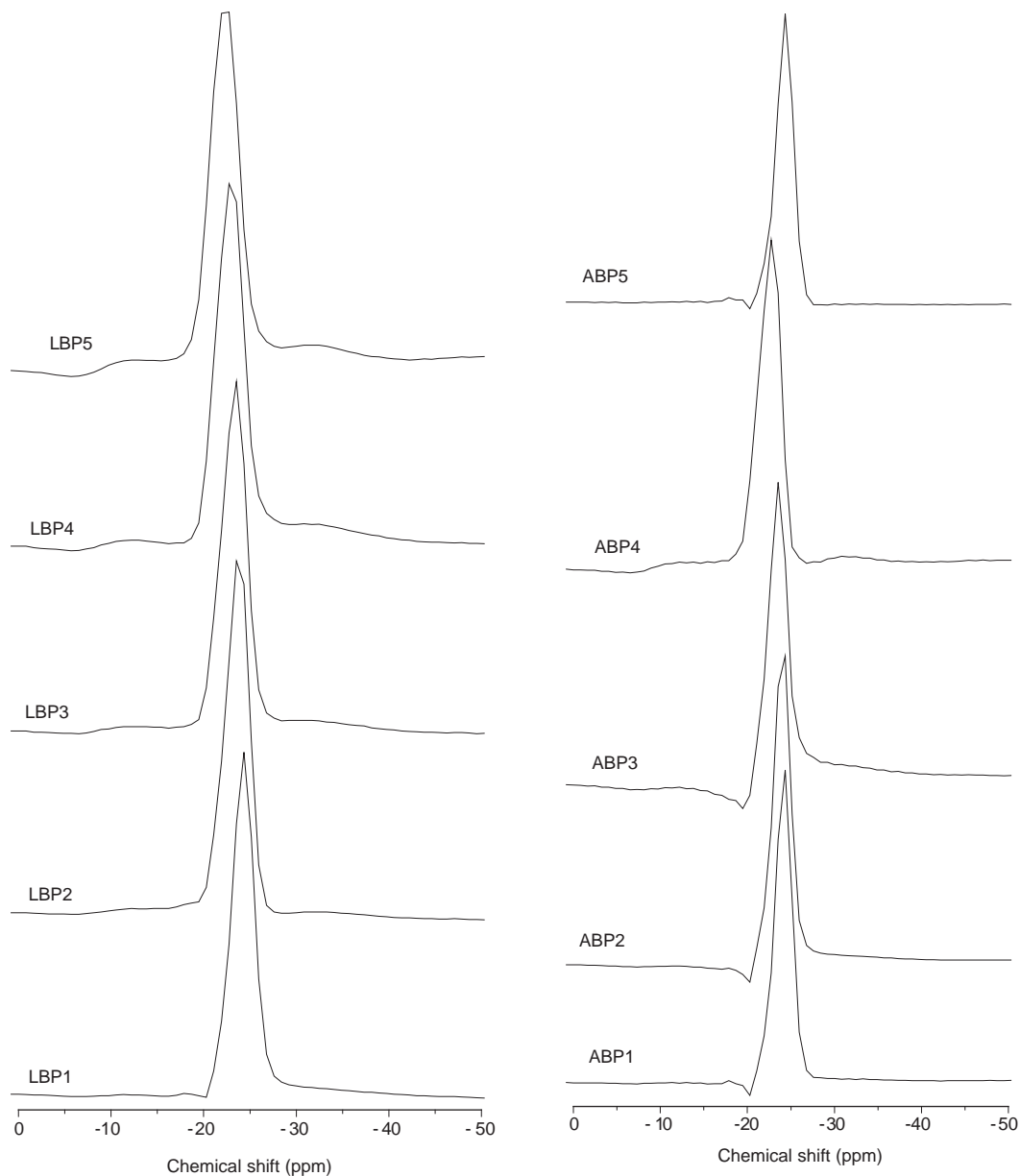
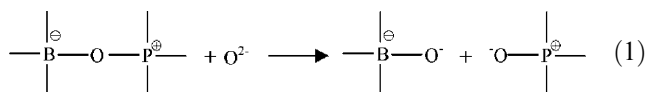


Fig. 5.  $^{11}\text{B}$  MAS NMR spectra of LBP and ABP glasses.

### 3.6. Structural model

We noted in passing that in the present glasses, the network formers  $\text{B}_2\text{O}_3$  and  $\text{P}_2\text{O}_5$  are in equal proportions and therefore would most likely form a borophosphate network. The ideal, hypothetical  $\text{BPO}_4$  glass would consist of a network of  $\text{BO}_4^-$  and  $\text{PO}_4^+$  units analogous to  $\text{SiO}_4$  network, with the additional feature of chemical ordering of the two basic structural units. Chemical ordering implies that each  $\text{P}_4^+$  unit is connected to four  $\text{B}_4^-$  units and each  $\text{B}_4^-$  unit is connected to four  $\text{P}_4^+$  units and only B–O–P linkages are present in the structure. This is visualized in Fig. 12(a). Since this is consistent with the earlier

reported work [4], we start with the chemically ordered tetrahedral network of a hypothetical  $\text{BPO}_4$  glass as the starting point for our discussion. Addition of  $\text{Li}_2\text{O}$  or  $\text{Ag}_2\text{O}$  acts as a modifier of such a network. Since network consists of only B–O–P linkages, the first stage of modification is uniquely defined,



( $\oplus$  and  $\ominus$  symbols are used to differentiate the formal charges present on the units from the charge created during modification). R.H.S. of Eq. (1) suggests that  $[\text{BO}_{4/2}]^-$  ( $\equiv \text{B}_4^-$ ) has been converted into  $[\text{BO}_{3/2}\text{O}]^{2-}$ .



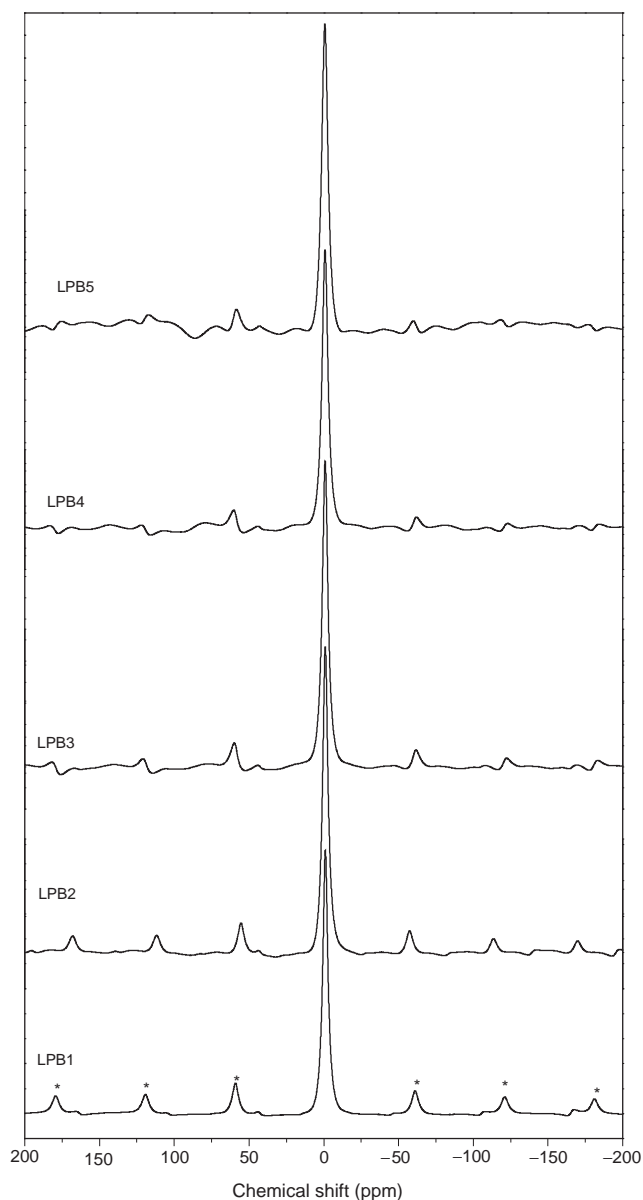


Fig. 6.  $^7\text{Li}$  MAS NMR spectra of LBP glasses.

But  $\text{B}_4^-$  has never been known to be associated with an NBO. On the other hand, when  $\text{P}_4^+$  is converted into  $[\text{P}^\oplus\text{O}_{3/2}\text{O}]^-$ , it is readily reverted to  $[\text{POO}_{3/2}]^0$ . It is easy to visualize the formation of ultraphosphate unit in the structure form  $[\text{P}^\oplus\text{O}_{3/2}\text{O}]^-$  because it possesses the same reduced connectivity of three in the structure as  $[\text{POO}_{3/2}]^0$ . The product species on the R.H.S. of Eq. (1) are significantly different in their group electronegativities [31]. Therefore they can be expected to react with each other and reform their structures [31–33]. The electronegativities of  $[\text{BO}_{3/2}\text{O}]^{2-}$  and  $[\text{POO}_{3/2}]^0$  being 1.44 and 3.02, respectively, the possible reaction can be visualized as



The electronegativities of the products  $[\text{BO}_{4/2}]^-$  and  $[\text{POO}_{2/2}\text{O}]^-$  are 2.01 and 2.39, respectively, and these values lie between the electronegativities of the reactants. The reaction is, therefore, considered as chemically feasible [34]. Reaction (2) implies that boron is restored in its original tetrahedral structure, while the modifier has affected only the phosphate moiety. Thus both the NBOs formed as a result of modification are passed onto the phosphate unit and the number of covalent connections in the network is reduced by two. In the process, a 4-connected  $\text{P}_4^+$  unit has become two connected  $[\text{POO}_{2/2}\text{O}]^-$  unit. For the chemically ordered structure of the glass, it only means that after modification there are not enough BOs emanating from phosphate units to satisfy the BO requirements of the (unaffected)  $\text{B}_4^-$  units. This entails the formation of B–O–B bonds in place of B–O–P bonds in the structure, which produces links between tetrahedral borons.

Such a modification process as described above can continue till all the  $\text{P}_4^+$  units are converted to  $[\text{POO}_{2/2}\text{O}]^-$  ( $\equiv \text{P}_2^-$ ) units. This happens when compositions corresponding to LBP5 and ABP5 glasses are arrived at because there is 50 mol%  $\text{Li}_2\text{O}$  and 50 mol%  $\text{Ag}_2\text{O}$ , respectively, in these glasses. We may quantify the effect of modification and calculate the different structural units in the glass compositions on the basis of the suggested process of modification. We may note that a unit  $\text{B}_2\text{O}_3$  leads to  $2\text{B}_4^-$  units and a unit of  $\text{P}_2\text{O}_5$  leads to  $2\text{P}_4^+$  units. In LBP1 and ABP1 glasses, there are 70  $\text{B}_4^-$  and 70  $\text{P}_4^+$  units to start with and 30  $\text{Li}_2\text{O}$  has been added. We therefore expect 30  $\text{P}_4^+$  units to be converted into 30  $\text{P}_2^-$  units, while 70  $\text{B}_4^-$  units are left unaffected in both LBP1 and ABP1 glasses. However, B–O–B bonds are formed by a new inter  $\text{B}_4^-$  connections. For this purpose, 60 of the 70  $\text{B}_4^-$  units have to be interconnected through one B–O–B bond each. In the case of LBP5 or ABP5 glass, where all of  $\text{P}_4^+$  units are converted into  $\text{P}_2^-$  units, the 50  $\text{B}_4^-$  tetrahedra have to make 100 B–O–B bonds (two each on an average), which imply formation of connected chains of tetrahedral  $\text{B}_4^-$  units. In the ideal situation, where all  $\text{B}_4^-$  units are similarly and uniformly connected to two other  $\text{B}_4^-$  units, it results in a very fascinating structure, in which chains of  $\text{B}_4^-$  units are formed and the chains themselves are interconnected through metaphosphate units as visualized in Fig. 12(b). This idealized structure can be quite stable unless it is perturbed by the polarizing effect of the highly polarizing (high  $e/r$ , where  $e$  is the charge and  $r$  is the radius)  $\text{Li}^+$  ions. The latter prefers to occupy tetrahedrally coordinated positions surrounded by NBOs and in the process converts  $[\text{BO}_{4/2}]^-$  units into the chemically equivalent  $\text{B}_2^-$  ( $\equiv [\text{BO}_{2/2}\text{O}]^-$ ) units. The effect of this on the topology of the structure can be quite deleterious.  $\text{B}_4^-$ – $\text{B}_2^-$  conversion results in a drastic reduction of the number of covalent connections (from 4 to 2). Indeed this appears to happen in  $\text{Li}_2\text{O}$  rich LBP glasses because,

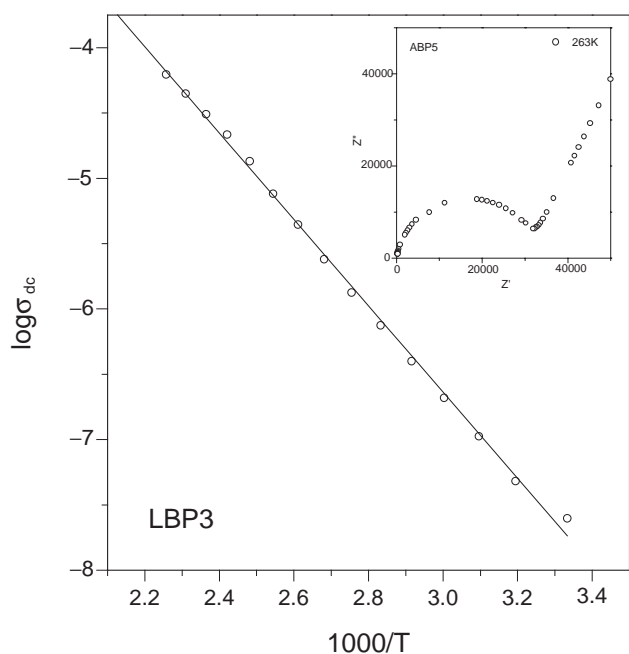


Fig. 7. Arrhenius plot of DC conductivities of ABP3 glass. The solid line in the figure is the best fit line. The inset shows (typical) Nyquist plot for the ABP5 glass at 263 K.

Table 4

DC conductivity ( $\sigma_{dc}$ ), activation barriers ( $E_{dc}$ ) and  $\sigma(0)$  obtained from Power law fits of AC conductivity data

Glass	$\sigma_{dc}^a$	$E_{dc}$ (eV)	$\sigma(0)$
LBP1	$1.07 \times 10^{-8}$	0.75	$9.93 \times 10^{-8}$
LBP2	$3.50 \times 10^{-7}$	0.70	$3.22 \times 10^{-7}$
LBP3	$1.38 \times 10^{-6}$	0.66	$1.33 \times 10^{-6}$
LBP4	$3.87 \times 10^{-6}$	0.60	$3.75 \times 10^{-6}$
LBP5	$1.28 \times 10^{-5}$	0.57	$1.20 \times 10^{-5}$
ABP1	$4.88 \times 10^{-7}$	0.59	$4.27 \times 10^{-7}$
ABP2	$2.68 \times 10^{-6}$	0.59	$2.44 \times 10^{-6}$
ABP3	$8.70 \times 10^{-6}$	0.52	$8.19 \times 10^{-6}$
ABP4	$8.40 \times 10^{-5}$	0.36	$8 \times 10^{-5}$
ABP5	$2.89 \times 10^{-4}$	0.37	$3.00 \times 10^{-4}$

<sup>a</sup>The conductivities refer to 363 K.

concentration  $B_3$  ( $= 1 - N_4$ ) observed from NMR seems to increase (Table 3)).  $B_4^- \rightarrow B_2^-$  conversion is much smaller in ABP glasses as a result of which  $B_4^-$  concentration remains essentially unaffected (Table 3). On the basis of the model, it is possible to calculate the numbers of  $B_4^-$  units, which are variously connected to other  $B_4^-$  units as a function of composition. Assuming total of 100 molecular units ( $n_1Li_2O \cdot n_2B_2O_3 \cdot n_2P_2O_5$ , with  $n_1 + 2n_2 = 100$ ), the number of such units has been calculated. Their variation as a function of  $M_2O$  ( $Li_2O$  or  $Ag_2O$ ) is shown in Fig. 13. Number for  $P_4^+$  and  $P_2^-$  species calculated similarly are also listed in Table 3. It is interesting to note that in the composition regime we have investigated, (30–50% of  $Li_2O/Ag_2O$ ), the concen-

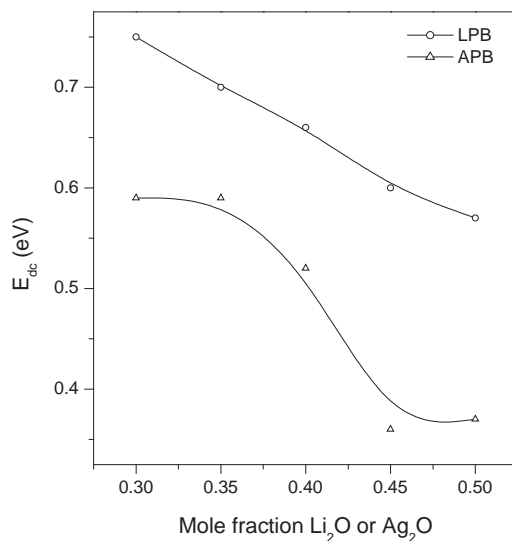
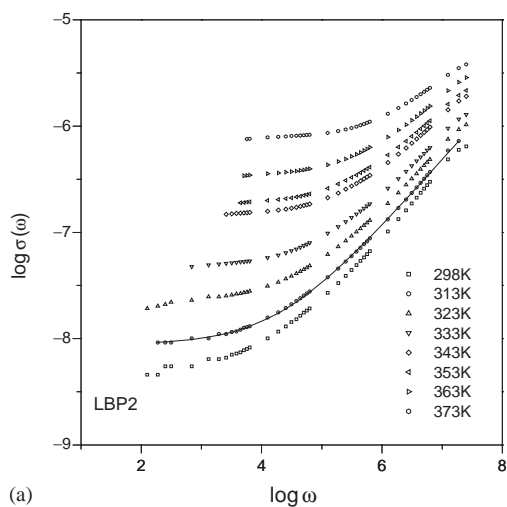


Fig. 8. The variation of activation barrier ( $E_{dc}$ ) as a function of modifier oxide concentration.

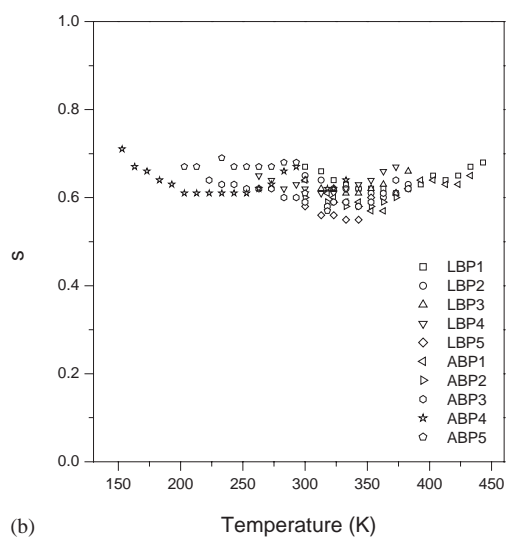
trations of isolated  $B_4^-$  units vanish and singly connected (pairs)  $B_4^-$  pass through a maximum and decreases rapidly towards zero. But the concentration of 2-connected  $B_4^-$  units, which forms  $B_4^-$  chains increase continuously and rapidly. We discuss below the various observed properties on the basis of above structural model.

#### 4. General

Molar volumes decrease in both LBP and ABP series of glasses as the modifier concentration increases. But the variation is almost linear in LBP series, while in ABP glasses, the variation has two slopes with two knees around 35 mol% and 45 mol%  $Ag_2O$ . While molar volume decrease in both systems is partly due to linear decrease in the quantities of the glass formers, it is also partly attributable to the partial collapse of the ideal borophosphate structure due to  $P_4^+ \rightarrow P_2^-$  conversion. We speculate that even as the  $B_4^-$  units get progressively interconnected through B–O–B bridges,  $Li_2O$  in LBP compositions may also induce  $B_4^- \rightarrow B_2^-$  conversion as it wont [35]. The probability of the conversion increases with the concentration of  $Li_2O$  and may increase linearly with  $Li_2O$  concentration. Therefore, the variation of molar volume in the composition regime investigated here is quite linear in LBP glasses. The extrapolation of molar volumes (inset to Fig. 1 (b)) towards 0 mol fraction of  $Li_2O$  corresponds to the molar volume of the hypothetical borophosphate (BP) glass and is equal to  $\sim 42.20 \text{ cm}^3$ . This may be compared with the molar volume of  $38.33 \text{ cm}^3$  of crystalline  $BPO_4$ . If we assume  $P_4^+$  and  $B_4^-$  tetrahedra have molar volumes of 10.92 and  $8.17 \text{ cm}^3$  respectively (arrived at by assuming the radii of



(a)



(b)

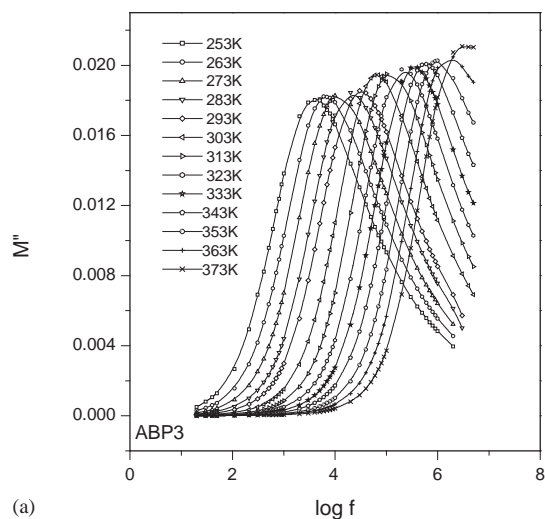
Fig. 9. (a) Almond-West plots of AC conductivity at various temperatures of LBP2 glass and power law fitting is also shown for the data at 313 K. (b) Variation of  $s$  as a function of temperature for all the glasses.

Table 5

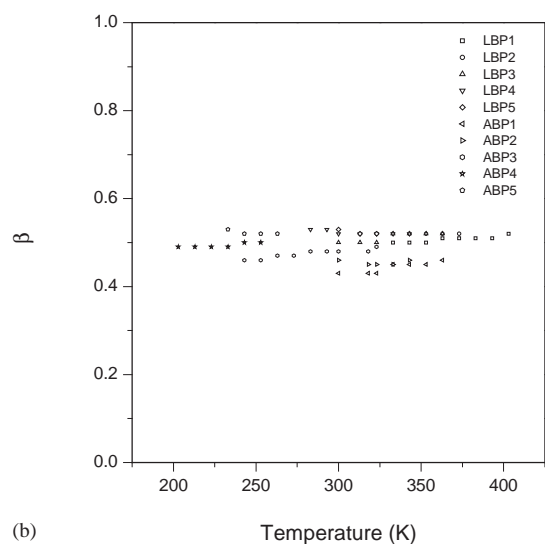
Power law fit parameters along with  $\beta$  values at various temperatures for LBP2 glass

$T$ (K)	$\sigma(0)$	$A$	$s$	$\chi^2$	$\beta$
298	$4.85 \times 10^{-9}$	$1.08 \times 10^{-11}$	0.65	0.00026	0.52
313	$8.66 \times 10^{-9}$	$1.63 \times 10^{-11}$	0.64	0.00011	0.52
323	$2.17 \times 10^{-8}$	$2.63 \times 10^{-11}$	0.62	0.00002	0.52
333	$4.60 \times 10^{-8}$	$3.62 \times 10^{-11}$	0.62	0.00001	0.52
343	$1.40 \times 10^{-7}$	$5.34 \times 10^{-11}$	0.62	0.00004	0.52
353	$1.75 \times 10^{-7}$	$7.09 \times 10^{-11}$	0.61	0.00003	0.52
363	$3.22 \times 10^{-7}$	$1.01 \times 10^{-10}$	0.60	0.00002	0.52
373	$7.37 \times 10^{-7}$	$1.07 \times 10^{-10}$	0.61	0.00006	0.52

$B_4^-$  and  $P_4^+$  units as 1.48 and 1.63 Å respectively). The random close packing (rcp) volume of  $BPO_4$  glass would be 31.30 cm<sup>3</sup>. The rcp glass [1] has thus a significantly lower volume suggesting a rather open network of



(a)



(b)

Fig. 10. (a) Variation of  $M''$  as a function of  $\log f$  for ABP3 glass at various temperatures and (b) the variation of  $\beta$  as a function of temperature for all the glasses.

corner sharing tetrahedra of the glasses. At the other extreme of extrapolation, we get a molar volume of 14.20 cm<sup>3</sup> for the hypothetical  $Li_2O$  glass, which is lower than its crystalline volume (14.85 cm<sup>3</sup>). In the case of ABP glasses, we observe a knee in the region of 35 mol%  $Ag_2O$  and another knee in the opposite direction around 45 mol%  $Ag_2O$ . Although it appears unusual, extrapolation beyond the second knee towards  $Ag_2O$  end gives a nearly correct molar volume of hypothetical  $Ag_2O$  glass of  $\sim 34.00$  cm<sup>3</sup> compared to crystalline value of 32.18 cm<sup>3</sup>. However, glass formation is difficult above 50%  $Ag_2O$  and therefore, the extrapolation itself is based on insufficient data points. On a closer examination along with Fig. 13, it appears that the compositions corresponding to the knees occur, where the concentrations of (1) isolated and two connected  $B_4^-$

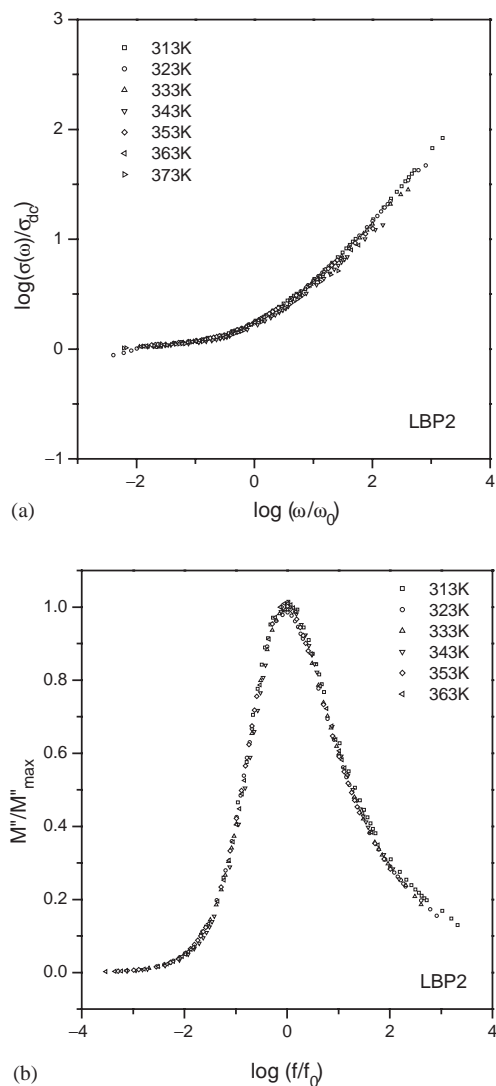


Fig. 11. (a) Reduced AC conductivity plots for and (b) the reduced  $M''$  plot for LBP2 glass.

species and (2) singly connected and two connected  $B_4^-$  species intersect. On this basis we are led to speculate without additional proof that coexistence of equal numbers  $B_4^-$  units in isolation and in  $B_4^-$  chains in the structure causes destabilization and therefore they tend to reorganize. During the process some of the  $B_4^-$  units may transform to  $B_2^-$ . In the region of 40–45 mol%  $Ag_2O$ , where the concentration of  $B_4^-$  units in pairs and in chains are similar, they tend to stabilize each other by promoting formation of chains from  $(B_4^-)_2$  pairs. Therefore the rapidly decreasing trend of volume is arrested. The nature of volume variation also indicates that there may not be any further degradation of  $B_4^-$  tetrahedra.

The NMR measurements qualitatively support the above observations. We may note here parenthetically that magnitude of chemical shifts is affected by the

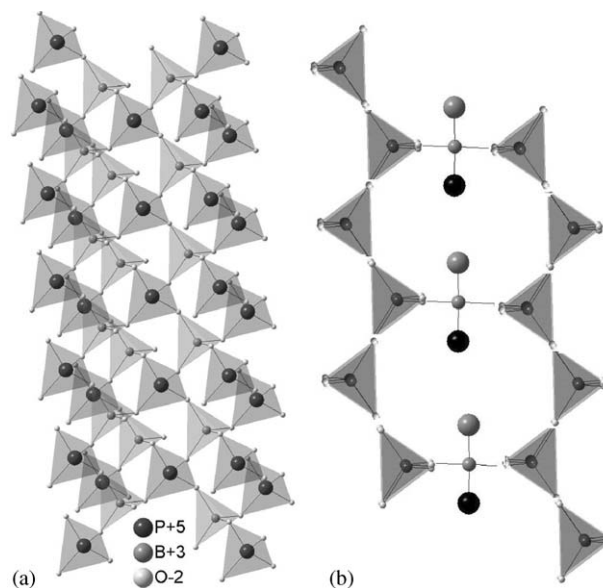


Fig. 12. (a) Structure of chemically ordered hypothetical  $BPO_4$  glass and (b) structure of highly modified borophosphate glass consisting of  $B_4^-$  chains interleaved by metaphosphate units.

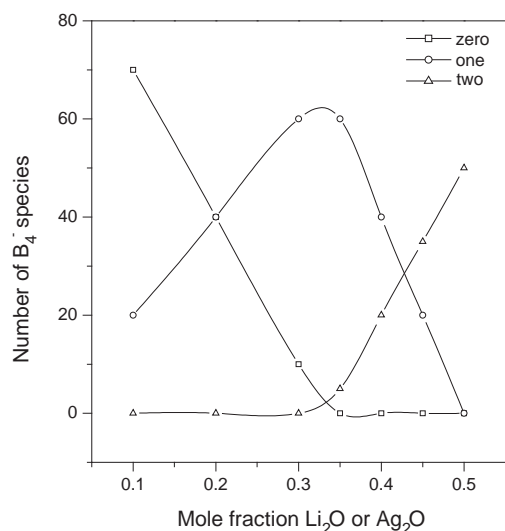


Fig. 13. The variation of the number of  $B_4^-$  species having zero, one and two B–O–B connections as a function of modifier concentration (in  $n_1Li_2O/Ag_2O \cdot n_2B_2O_3 \cdot n_3P_2O_5$ , where  $n_1 + n_2 + n_3 = 100$ ).

polarizing power of the cations.  $Z/r$  values of  $Li^+$  ions being higher than the same for  $Ag^+$  ions, the phosphorus chemical shifts are generally less deshielded in the case of  $Ag^+$  containing glasses (see Ref. [1]). As indicated in Table 3, there is only one  $^{31}P$  broad signal in LBP glasses. We should expect the presence of two types of phosphorus from Table 3, one from  $P_4^+$  units and the other from  $P_2^-$  units. But they appear to be convoluted into a single peak. With increasing  $Li_2O$ , the concentration of  $P_4^+$  species decreases and that of  $P_2^-$  increases. Correspondingly, the chemical shift values change

gradually from  $-19$  to  $-2$  ppm. Since all  $P_2^-$  species are isolated by intervening  $B_4^-$ , according to the above model the chemical shift values of  $^{31}P$  in such isolated units appears to be approximately  $-2$  ppm. Chemical shifts corresponding to the peaks actually represent weighted contributions of  $P_4^+$  and  $P_2^-$  convoluted into a common peak. Extrapolation towards hypothetical  $BPO_4$  glass suggest a chemical shift of  $-43$  ppm for  $P$  in  $P_4^+$ , more deshielded than in  $[POO_{3/2}]^0$  units. This is consistent with higher partial charge on the phosphorus  $+0.719$  in  $P_4^+$  compared to  $+0.360$  in  $[POO_{3/2}]^0$  as calculated approximately using Sanderson's method [31]. The chemical shift value of  $-2.0$  ppm of  $P_2^-$  is also similarly consistent with the partial charge of  $+0.087$  on the phosphorus. As noted earlier,  $B_4^- \rightarrow B_2^-$  conversion, which occurs due to the presence of  $Li_2O$  is borne out by the observed increasing concentration of  $B_3$  units in LBP2 to LBP5 glasses. (The quadrupolar split  $B_3$  resonance appears as wings at the base of the dominant  $B_4$  peak.) In Table 3,  $N_4$  values decrease and therefore  $B_3$  concentration ( $=1-N_4$ ) increases towards LBP5 glass. In ABP glasses, the behavior of the main resonance peak is similar to that in LBP glasses, but there appears to be clear evidence of two resonance peaks in ABP4 and ABP5 glasses. Both minor resonances indicate more shielded  $^{31}P$  nucleus and suggestive of the formation of pyrophosphate units. This is possible only if  $Ag_2O$  reacts with already existing metaphosphate rather than  $P_4^+$  units. This is possible only if the  $Ag^+$  ions and  $O^{2-}$  ions from the added  $Ag_2O$  are preferentially driven to the more flexible and open spaces, which exist near metaphosphate units in the structure, which promotes such a reaction. Pyrophosphate units are chain terminators and their formation help local reorganization, which stabilizes  $B_4^-$  units in the structure. This is corroborated by the fact that there are hardly any  $B_3$  units in ABP glasses except in ABP5 composition (Table 3). The chemical shifts of  $^7Li$  from Table 3 indicates that  $^7Li$  gets progressively shielded, although to a small extent as  $Li_2O$  concentration is increased. This is again consistent with the role of  $Li_2O$ , which seeks close coordination of NBO's in the structure and this shifts the  $^7Li$  resonance towards more shielded values.

Glass transition temperatures decrease in both LBP and ABP series of glasses as a function of mole fraction of modifier. But the decrease is much smaller in  $Li_2O$  modified glasses compared to  $Ag_2O$  modified glasses. Since  $Li_2O$  promotes to some extent  $B_4^- \rightarrow B_2^-$  conversion and acquires a tight coordination of NBO's, there is a tightening of the glass network. This manifests in reducing the otherwise rapid fall of  $T_g$ 's. But the  $Ag^+$  ions do not behave the same way as  $Li^+$ . Also formation of pyrophosphate units by localized 'overmodification' ( $P_2^-$  to  $P_1^-$ ) in ABP glasses noted above weakens the network structure. This results in a severe fall in  $T_g$

values as  $Ag_2O$  concentration increases. There may be other reasons for the observed trends in  $T_g$ . The total cohesive energies of ABP glasses to a first approximation (assuming additivity of cohesive energies) are lower than those of LBP glasses, because the cohesive energy of  $Li_2O$  is greater than that of  $Ag_2O$ . Therefore, the melting temperatures and glass transition temperatures can be expected to be lower for ABP glasses than in LBP glasses. Further,  $T_g$ 's of modified glasses can be directly related to the cage vibrational frequencies of mobile ions in the cluster model of glasses [36–37]. The cage vibrational frequency of  $Li^+$  ion ( $\sim 400$ – $450$   $cm^{-1}$ ) is significantly higher than that of  $Ag^+$  ion ( $\sim 100$ – $150$   $cm^{-1}$ ). But the cage vibrational frequencies of  $Li^+$  and  $Ag^+$  ions have not been determined in these glasses. However, the  $T_g$ 's of the two series of glasses are nearly equal around 30 mol% modification and the  $T_g$  behavior below 30 mol% modification has not been examined. It would be tempting to conclude that  $T_g$  of the two series of glasses could be very similar below 30% modification because a large percentage of  $P_4^+$  units are still intact in these compositions and the rigidity of the networks, which determines the  $T_g$  values are similar. From Table 2, we also notice that the  $\Delta C_p$  values are high in both the series of glasses, consistent with the high degree of ionic bonding. They are also slightly higher in ABP glasses than in LBP glasses because of the additional "at-no-cost" degradation ( $B_4^- \rightarrow B_2^-$ ), which  $Li_2O$  causes as a result of which the average ionic bonding increases in LBP glasses. Thermodynamic fragilities ( $F_{1/2}$ ) are also in the 50% range for all the glasses, which are typical of modified network glasses. This range of  $F_{1/2}$  suggest significant VTF behavior in the molten state, consistent with the possibility of large size of cooperatively rearranging regions (CRR) due to the formation of  $B_4^-$  chains as  $T_g$  is approached.

Infrared spectra of Fig. 3 of the two glass series also bear out the essential features of the proposed structural model. Since the very first LBP composition already contains 30%  $Li_2O$ , there are already  $P_2^-$  units, which give rise to  $P=O$  vibration in the region of  $1200$   $cm^{-1}$ . Also, they do not form an uninterrupted phosphate chain and the NBO in  $P_2^-$  is in the coordination of the nearby  $Li^+$  ions,  $P=O$  vibrations persist even at these high levels of modification. Their relative intensities increase towards LBP5. The  $\sim 1000$   $cm^{-1}$  peak may arise from the asymmetrical stretching in the phosphate tetrahedra in  $P_4^+$  units and it vanishes gradually as expected towards LBP5 glass. Also as  $Li_2O$  concentration increases,  $P-O-B$  links decrease in number and the corresponding vibrational frequency is also slightly blue shifted. This is consistent with the gradual  $P_4^+ \rightarrow P_2^-$  conversion and the comfortable positioning of  $P_2^-$  units between  $B_4^-$  units. There seems to be no absorption features in the  $1400$   $cm^{-1}$  region, although it is partly blurred by the noise. This confirms virtual absence of  $B_3$



units. However, there is a slight intensity build up towards LBP5. All vibrational features arising from  $B_4^-$  tetrahedra are buried in the broad peak in the region of  $1000\text{ cm}^{-1}$  region. ABP glasses exhibit very similar features except that in ABP5 there is additional absorption feature (4 clear sub-peaks between  $800$  and  $1200\text{ cm}^{-1}$ ) in which  $\sim 850\text{ cm}^{-1}$  feature can be attributed to the formation of pyrophosphate unit. Similarly formation of  $B_2^-$  units corresponding to trigonal boron which was found to be present in the  $^{11}\text{B}$  MAS NMR of ABP5 glass also shows up clearly in the split peak between  $1300$  and  $1400\text{ cm}^{-1}$ . The origin of  $B_2^-$  is evidently due to some amount of reorganization leading to  $B_4^-$  to  $B_2^-$  conversions in highly modified ABP5 glass.

#### 4.1. Ion transport studies

DC activation energies ( $E_{dc}$ ) of both LBP and ABP glasses decrease as modification is increased. Conventionally, this would appear as due to the opening up of the channel like space between chains of  $B_4^-$  tetrahedra, which allows less hindered motion of  $\text{Li}^+$  and  $\text{Ag}^+$  ions. But such spaces are interrupted by the presence of  $P_4^+$  and  $P_2^-$  units. There is also a gradual decrease in molar volume, which leads to a contraction of the open space. Therefore,  $E_{dc}$  should have increased. But the observed decrease in activation barrier is indicative of a different mechanism of ion transport, which we have examined recently in several modified network oxide glasses. We suggest that there are two successive steps in conduction, first the migration of an NBO via NBO–BO switching and second the follow up motion of the cation ( $\text{Li}^+$  or  $\text{Ag}^+$  in the present case). NBO–BO switching involves an intermediate high-energy stage, where the network atom is over coordinated and its orbitals are rehybridized. This high-energy state determines the observed  $E_{dc}$ . The cation motion has a lower barrier and does not manifest in the measurements of  $E_{dc}$ . But it is associated with a polarization that relaxes with characteristic time constant and causes broadening of the relaxation peaks. Therefore, the decrease in  $E_{dc}$  is due to increased facility of NBO–BO switching. This can occur as long as there is a contiguity of BO's and NBO's in the structure irrespective of their actual numbers. In the present case, there is a gradual increase in the concentration of  $P_2^-$  species.  $P_2^-$  ( $\equiv[\text{POO}_{2/2}\text{O}]^-$ ) is two connected and can easily librate (swing). The swinging NBO can interact readily with BO on a neighboring phosphate or borate unit to enable NBO–BO switching [38,39]. This becomes more and more facile when greater number of NBO's are present in the system, particularly in the channel like space between strands of  $B_4^-$ . We would therefore expect activation barriers to decrease as indeed observed in these glasses. Because of the higher ionic potential of  $\text{Li}^+$  ions, the freedom of libration of the  $P_2^-$  units is somewhat curtailed, which therefore

keeps the activation barriers in LBP glasses higher than in ABP glasses.

In ABP glasses, the activation barriers are low for yet another reason, their molar volumes are high and the activated state during BO–NBO switching is more easily accommodated, which decreases the barriers significantly. The presence of an intact  $\text{BPO}_4$  network at the low levels of modification may lead to near constancy of activation barriers (Fig. 8) as it happens in the case of molar volumes. The leveling off of the activation barriers at high percentages of  $\text{Ag}_2\text{O}$  may be again due to the effect of low sensitivity of molar volumes; the molar volumes of the glasses in this region are determined by  $\text{Ag}_2\text{O}$  itself.

The AC conductivities reveal an important feature and that is the presence of a nearly constant  $s$ , which is independent of composition and temperature and even the cation. This is clearly suggestive of the AC response arising from one unchanging chemical or physical feature of the glasses. We consider this to be the NBO–BO switching present in all the glasses. NBO–BO switching is involved in the transport of both charge (DC conductivities) and polarization (AC conductivities). The AC conductivity master plot (Fig. 11(a) confirms good collapse of reduced conductivities (with modest spread at high frequencies), which is again suggestive of a common AC conductivity mechanism, which we propose as the NBO–BO switching followed by cation migration.

The modulus ( $M''$ ) peaks do not all have the same amplitude, although the spread of the maximum values is very small over the entire temperature span of  $120^\circ$ .  $\beta$  values determined for all the glasses both LBP and ABP over  $200^\circ$  span of temperature also reveal a near constant value of  $\beta$  (Fig. 10 (b)). We feel that the origin of  $\beta$  itself is because of a two component polarization relaxation, the first component is associated with the NBO in its new position and the polarization around it and the second component is that associated with the cation, which occurs after a time delay (the cation moves to the new position after a delay). That a common  $\beta$  is observed is suggestive of the close similarity of the mechanism and magnitudes of delay—delay time is most effective in determining  $\beta$  values [40]. The reduced plots of  $M''/M''_{\max}$  vs  $\log(f/f_0)$  also reveal excellent collapse, suggesting the validity of time–temperature superposition, which again points towards the presence of a single operative mechanism for dielectric relaxation.

## 5. Conclusions

Lithium borophosphate and silver borophosphate glasses have been investigated using a number of experimental techniques. Ion transport has been studied over a wide range of frequencies and temperatures. It is found that the observed properties are consistent with a



model, which considers the modification of initial  $\text{BPO}_4$  units by the addition of  $\text{Li}_2\text{O}$  or  $\text{Ag}_2\text{O}$ . Structural consequence of modification is quite interesting.  $[\text{BO}_4]^-$  units of the glass remains essentially unaffected and  $[\text{PO}_4]^+$  is continuously converted into metaphosphate  $[\text{POO}_{2/2}\text{O}]^-$  units. The modification behavior of  $\text{Li}_2\text{O}$  and  $\text{Ag}_2\text{O}$  exhibit nontrivial differences. Higher DC conductivities and lower activation barriers are found to be associated with ABP glasses compared to LBP glasses. AC conductivities exhibit simple power law variation. Both AC conductivities and moduli ( $M''$ ) have been found to be collapsible on to master plots, suggesting the presence of a common charge transport mechanism in these glasses. The proposed structural model consistently accounts for all the observations made in the present investigation.

## References

- [1] K.J. Rao, Structural Chemistry of Glasses, Elsevier, Amsterdam, 2002.
- [2] M. Scagliotti, M. Villa, G. Chiodelli, J. Non-Cryst. Solids 93 (1987) 350.
- [3] M. Scagliotti, M. Villa, G. Chiodelli, G., J. Non-Cryst. Solids 94 (1987) 101.
- [4] Y.H. Yun, P.J. Bray, J. Non-Cryst. Solids 30 (1978) 45.
- [5] N.K. Kreidl, W.A. Weyl, J. Am. Ceram. Soc. 24 (1941) 372.
- [6] K. Takahashi Advances in Glass Technology, Proceedings of the 6th International Congress on Glass, Washington DC, Plenum Press, New York, 1962.
- [7] L.D. Bogomolova, V.A. Zhachkin, V.N. Lazukin, N.F. Shapovalova, V.A. Shmukler, Sov. Phys. Dokl. 16 (1972) 967.
- [8] D.F. Ushkov, N.F. Baskova, Yu.P. Tarlakov, Fizika i Khimiya Stekla 1 (1975) 151.
- [9] L. Koudelka, P. Mosner, Mater. Lett. 42 (2000) 194.
- [10] L. Koudelka, P. Mosner, J. Non-Cryst. Solids 293–295 (2001) 635.
- [11] J.F. Duce, J.J. Videau, M. Couzi, Phys. Chem. Glasses 34 (1993) 212.
- [12] J.F. Duce, J.J. Videau, K.S. Suh, J. Senegas, Phys. Chem. Glasses 35 (1994) 10.
- [13] A. Magistris, G. Chiodelli, M. Villa, J. Power Sources 14 (1985) 87.
- [14] G. Chiodelli, A. Magistris, M. Villa, Solid State Ion. 18&19 (1986) 356.
- [15] K. Ito, C.T. Moynihan, C.A. Angell, Nature 398 (1999) 492.
- [16] D.E.C. Corbridge, E.J. Lowe, J. Chem. Soc. (1954) 493.
- [17] R.M. Almeida, J.D. Mackenzie, J. Non-Cryst. Solids 40 (1980) 535.
- [18] J.J. Hudgens, S.W. Martin, J. Am. Ceram. Soc. 76 (1993) 1691.
- [19] D.P. Almond, G.K. Duncan, A.R. West, Solid State Ion. 8 (1983) 159.
- [20] D.P. Almond, C.C. Hunter, A.R. West, J. Mater. Sci. 19 (1984) 19, 3236.
- [21] D.P. Almond, A.R. West, R. Grant, J. Solid State Commun. 44 (1982) 1277.
- [22] A.K. Jonscher, Nature 267 (1977) 673.
- [23] R. Kohlrausch, Pogg. Ann. Phys. 12 (1847) 393.
- [24] G. Williams, D.C. Watts, Trans. Faraday Soc. 66 (1970) 80.
- [25] G. Williams, D.C. Watts, S.B. Dev, A.M. North, Trans. Faraday Soc. 67 (1971) 1323.
- [26] P.B. Macedo, C.T. Moynihan, R. Bose, Phys. Chem. Glasses 13 (1972) 171.
- [27] C.T. Moynihan, L.P. Boesch, N.L. Laberge, Phys. Chem. Glasses 14 (1973) 122.
- [28] B. Roling, A. Happe, K. Funke, M.D. Ingram, Phys. Rev. Lett. 78 (1997) 2160.
- [29] D.L. Sidebottom, P.F. Green, R.K. Brow, Phys. Rev. B 56 (1997) 170.
- [30] D.L. Sidebottom, Phys. Rev. Lett. 82 (1999) 3653.
- [31] R.T. Sanderson, Polar Covalence, Academic Press, New York, 1983.
- [32] S. Muthupari, K.J. Rao, J. Phys. Chem. 98 (1994) 2646.
- [33] S. Kumar, S. Murugavel, K.J. Rao, J. Phys. Chem. B 105 (2001) 5862.
- [34] L. Pauling, Nature of the Chemical Bond, Cornell University Press, New York, 1960.
- [35] S. Prabakar, K.J. Rao, C.N.R. Rao, Chem. Phys. Lett. 139 (1987) 96.
- [36] K.J. Rao, C.N.R. Rao, Mater. Res. Bull. 17 (1982) 1337.
- [37] K.J. Rao, Proc. Indian Acad. Sci. (Chem. Sci.) 93 (1984) 389.
- [38] M.H. Bhat, M. Ganguli, K.J. Rao, J. Phys. Chem. B, communicated.
- [39] K.J. Rao, S. Kumar, Curr. Sci. 85 (2003) 945.
- [40] S. Kumar, K.J. Rao, Chem. Phys. Lett., communicated.